SoftwareX 22 (2023) 101378

Contents lists available at ScienceDirect

SoftwareX

journal homepage: www.elsevier.com/locate/softx

Original software publication

An OpenFOAM solver for the extended Navier–Stokes equations

Johannes Schwarz [a,*], Kristjan Axelsson [a], Daniel Anheuer [a], Martin Richter [a], Johanna Adam [b], Martin Heinrich [b], Rüdiger Schwarze [b]

[a] Fraunhofer Institute for Electronic Microsystems and Solid State Technologies EMFT, Hansastr. 27d, 80686 München, Germany
[b] Institute for Mechanics and Fluid Dynamics, TU Bergakademie Freiberg, Lampadiusstr. 4, 09599 Freiberg, Germany

ARTICLE INFO

Article history:
Received 2 December 2022
Received in revised form 20 February 2023
Accepted 22 March 2023

Keywords:
Extended Navier–Stokes equations
OpenFOAM solver
Computational fluid dynamics
Microchannel flow

ABSTRACT

Classical continuum methods fail in predicting gas flows with higher Knudsen numbers. Several models have been derived in the past which extend the classical Navier–Stokes equations (CNSE) in order to capture the particle character of the medium. One approach takes into account the kinetic theory of gases. Accordingly, an additional self-diffusive mass flux can occur, which is a result of strong temperature and pressure gradients. These effects led to the derivation of the so called extended Navier–Stokes equations (ENSE). Under rare conditions they can be treated analytically. However, in most cases numerical methods are necessary. Usually the Finite-Volume-Method is utilized for numerically solving the CNSE, which is why the present work uses the well-known open-source-tool OpenFOAM as a foundation for developing an ENSE solver. It is pointed out that the advantage of being able to discretize certain terms implicitly and define additional diffusion face-flux fields leads to a huge performance gain in this case. Using a simple microchannel test case, the results are verified against analytical formulas.

© 2023 The Authors. Published by Elsevier B.V. This is an open access article under the CC BY license (http://creativecommons.org/licenses/by/4.0/).

Code metadata

Current code version	1.0
Permanent link to code/repository used for this code version	https://github.com/ElsevierSoftwareX/SOFTX-D-22-00403
Permanent link to Reproducible Capsule	
Legal Code License	GNU GPL V3
Code versioning system used	git
Software code languages, tools, and services used	C++
Compilation requirements, operating environments & dependencies	OpenFOAM v2006
If available Link to developer documentation/manual	
Support email for questions	johannes.schwarz@emft.fraunhofer.de

1. Motivation and significance

Common fluid flows are described using continuum approaches. The classical Navier–Stokes equations (CNSE) describe the conservation of mass, momentum and energy of a continuum. While this is viable from a macroscopic point of view, they fail to accurately predict gas flows through channels with small geometries and/or for rarefied-gas-flows. These kind of flows usually have Knudsen numbers above 0.001, which means that the continuum approach is not valid anymore and the medium has to be described as an ensemble of particles. That comes with disadvantages like a high computational effort, giving the motivation to use the CNSE and modify it to efficiently model such flows. One approach is the so called bi-velocity model by Brenner [1,2], which defines two conceptually different velocities. A numerical implementation of this model based on the OpenFOAM solver rhoCentralFoam was done by Christou and Dadzie [3]. Along with the use of Maxwell slip boundary conditions the results fit perfectly with the experimental data of Ewart

* Corresponding author.
E-mail addresses: johannes.schwarz@emft.fraunhofer.de (Johannes Schwarz), kristjan.axelsson@emft.fraunhofer.de (Kristjan Axelsson), daniel.anheuer@emft.fraunhofer.de (Daniel Anheuer), martin.richter@emft.fraunhofer.de (Martin Richter), johanna.adam@imfd.tu-freiberg.de (Johanna Adam), martin.heinrich@imfd.tu-freiberg.de (Martin Heinrich), ruediger.schwarze@imfd.tu-freiberg.de (Rüdiger Schwarze).

https://doi.org/10.1016/j.softx.2023.101378
2352-7110/© 2023 The Authors. Published by Elsevier B.V. This is an open access article under the CC BY license (http://creativecommons.org/licenses/by/4.0/).

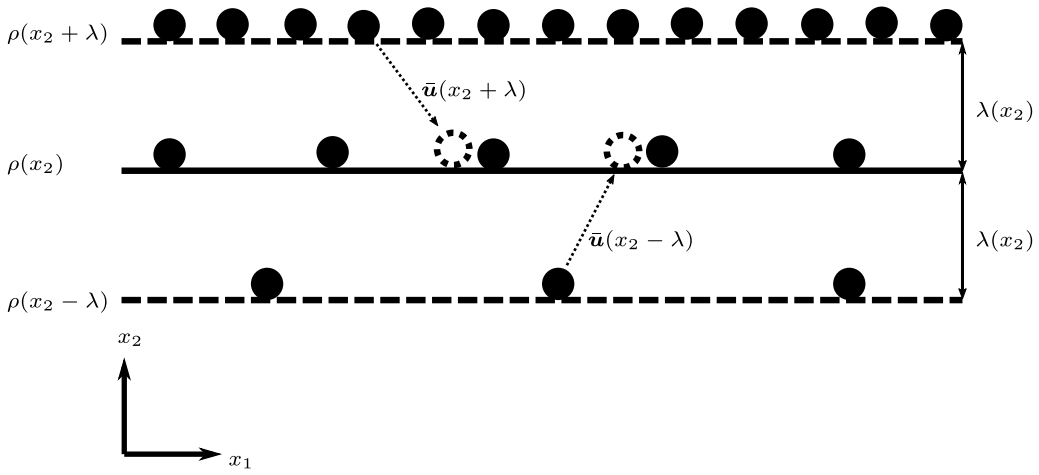


Fig. 1. Three hypothetical planes separated by a distance of the mean free path λ. Particles travel with $\bar{u}$ from the upper and the lower plane in any direction. Because ρ is higher on the upper plane, statistically more particles will travel from there to the middle plane.

et al. [4] for mean Knudsen numbers of up to 80. However, it comes with a few disadvantages: In order to obtain a convergent simulation of shock waves it was necessary for Greenshields and Reese [5,6] to include mass diffusion in the continuity equation. Same authors also pointed out the insufficient physical reasoning during the derivation. Another promising approach is based on first principles and was followed by Durst et al. [7–9]. Hereby the kinetic theory of gases is used to extend the CNSE by new terms to take self-diffusion of mass into account. In the present work, a solver for these extended Navier–Stokes equations (ENSE) is implemented in OpenFOAM and verified for a simple test case.

1.1. Theoretical foundation

It is argued in the approach of Durst et al. [7–9] that the conditions that appear in microchannel gas flows give rise to high pressure gradients, which cause a self-diffusive mass flux. In the following section, the derivation of this ENSE is shown very briefly. For a detailed derivation see Sambasivam [10]. Transient and gravity terms are not considered in the present work.

1.1.1. Diffusive transport of mass

The diffusive transport of a conserved quantity in an ideal gas can be explained based on the kinetic theory of gases. Accordingly, the gas is composed of particles which are moving evenly distributed into any direction, elastically collide with each other and travel by a distance of the mean free path λ between collisions. The velocity distribution is given by the Maxwell–Boltzmann distribution, from which a temperature dependent mean molecular velocity $\bar{u}$ can be derived. Fig. 1 shows three hypothetical planes separated by a distance of the mean free path. If either the density/pressure or the velocity/temperature on the upper or lower plane is different, the resulting mass flux in the middle plane is not zero. From those considerations a diffusive mass flux (density) $\dot{\boldsymbol{m}}^D$ at any location can be derived for an ideal gas [10]:

$$\dot{\boldsymbol{m}}^D = -\mu\left(\frac{1}{p}\nabla p - \frac{1}{2T}\nabla T\right). \tag{1}$$

With the pressure p, temperature T and the viscosity μ. By dividing it by the density ρ the diffusive velocity can be obtained:

$$\boldsymbol{u}^D = \frac{\dot{\boldsymbol{m}}^D}{\rho}. \tag{2}$$

The total velocity $\boldsymbol{u}$ shall be now the sum of the classical convective velocity $\boldsymbol{u}^C$ and the newly derived diffusive velocity $\boldsymbol{u}^D$

$$\boldsymbol{u} = \boldsymbol{u}^C + \boldsymbol{u}^D. \tag{3}$$

Inserting this expression in the stationary form of the classical continuity equation yields the extended continuity equation:

$$\nabla\cdot\left(\rho\boldsymbol{u}^C\right) = -\nabla\cdot\dot{\boldsymbol{m}}^D, \tag{4}$$

where the term on the RHS is new compared to the classical equation.

1.1.2. Diffusive transport of momentum

In a similar way an extended shear stress tensor can be derived when the mass flux is initially weighted with the convective velocity $\boldsymbol{u}^C$:

$$\begin{aligned}\underline{\boldsymbol{\tau}}^{\boldsymbol{ENSE}} = &-\mu\left(\nabla\boldsymbol{u}^C + (\nabla\boldsymbol{u}^C)^{\mathrm{T}}\right) + \frac{2}{3}\mu\nabla\cdot\boldsymbol{u}^C\underline{\mathbf{I}}\\ &+ \dot{\boldsymbol{m}}^D\boldsymbol{u}^C + \boldsymbol{u}^C\dot{\boldsymbol{m}}^D - \frac{2}{3}\dot{\boldsymbol{m}}^D\cdot\boldsymbol{u}^C\underline{\mathbf{I}},\end{aligned} \tag{5}$$

where terms that include the unity matrix $\underline{\mathbf{I}}$ are related to the fluid's compressibility. The first three terms are a known part of the classical Newtonian shear stress tensor, while the last three terms are newly derived and represent the transport of momentum by mass diffusion. The extended shear stress tensor is now inserted into the stationary CNSE momentum conservation equation:

$$\nabla\cdot\left(\rho\boldsymbol{u}^C\boldsymbol{u}^C\right) = -\nabla p - \nabla\cdot\underline{\boldsymbol{\tau}}^{\boldsymbol{ENSE}}. \tag{6}$$

1.1.3. Diffusive transport of energy

Following the same procedure a diffusive transport of heat $\dot{\boldsymbol{q}}^D$ can be derived:

$$\dot{\boldsymbol{q}}^D = -\kappa\nabla T + \dot{\boldsymbol{m}}^D e. \tag{7}$$

Hereby κ represents the thermal conductivity. With C_V being the specific heat capacity at constant volume, it is calculated as $\kappa = C_V\mu$. The first term is the (classical) Fourier heat transport and the second term the additional self-diffusive heat transport. The heat flux in the classical conservation equation for internal energy e is now simply replaced by this expression. However, for compressible flows it is common to solve a conservation equation for the total energy E^C, which is the sum of the internal

energy e and the kinetic energy E^C_{kin}. The conservation equation for the latter can be derived by first multiplying the momentum conservation Eq. (6) by the convective velocity $\boldsymbol{u}^C$. Now, by adding the equations for e and E^C_{kin}, the extended total energy equation can be obtained:

$$\nabla\cdot(\rho\boldsymbol{u}^C E^C) = -\nabla\cdot\dot{\boldsymbol{q}}^D + E^C_{kin}\nabla\cdot\dot{\boldsymbol{m}}^D - \nabla\cdot(p\boldsymbol{u}^C) - \nabla\cdot(\underline{\boldsymbol{\tau}}^{\boldsymbol{ENSE}}\cdot\boldsymbol{u}^C). \quad (8)$$

2. Software description

The solver rhoSimpleFoam of the open source CFD software package OpenFOAM v2006 is used as a foundation for numerically solving the stationary form of the ENSE, i.e. Eqs. (4), (6) and (8) for the unknowns p, $\boldsymbol{u}^C$ and e, respectively. Originally, this was conceived as a sequential, pressure-based solver for the stationary, compressible CNSE that uses the SIMPLE algorithm for pressure–velocity coupling. See Moukalled et al. [11] for a detailed explanation of the algorithm. Accordingly, for each flow variable a system of equations is solved separately and by doing outer iterations the components are coupled in an explicit manner. In contrast, several works regarding stationary simulation of microchannel flows have been done using rhoCentralFoam [3,12,13], a transient, sequential and density-based algorithm that uses a central flux evaluation scheme, originally developed for solving high-speed flows [14]. However, as microchannel flows are usually subsonic, this solver could be highly ineffective [15,16]. The present section explains how rhoSimpleFoam is modified in order to efficiently solve the ENSE. Crucial part of the solver process is the assembly of the system of linear equations, i.e. the coefficient matrix and a source vector for each equation that has to be solved (Step 2, 3, 4, 6 and 7 in Fig. 2). There are generally two ways of discretizing a spatial operator such as divergence or laplacian:

- Implicitly: Matrix coefficients are formed, this being generally the preferred way. Practically it can be achieved by using operators from the `fvm` namespace within the OpenFOAM framework.
- Explicitly: The discretization is done by taking values from previous outer iterations. Hereby values of the source vector are built. Usually this requires more outer iterations and underrelaxation in order to be stable and converge. Corresponding operators lie within the `fvc` namespace of OpenFOAM.

The applicability of the implicit operators is limited and it requires a bit more insight into how they work in order to use them properly. According to the OpenFOAM Programmers Guide [17] the `fvm::div` operator works in the following way: After integrating $\nabla\cdot(\boldsymbol{\Psi}\phi)$ over a control volume V_{KV}, applying the Gaussian rule and approximating the surface integrals one obtains

$$\int_{V_{KV}} \nabla\cdot(\boldsymbol{\Psi}\phi)\,dV = \oint_{\partial V_{KV}} \phi\,\boldsymbol{\Psi}\cdot d\boldsymbol{S} = \sum_f \phi_f\left(\boldsymbol{\Psi}^{n-1}_f\cdot\boldsymbol{S}_f\right) = \sum_f \phi_f \Phi^n_f, \quad (9)$$

where $\boldsymbol{\Psi}$ is an arbitrary vector and ϕ the variable that is being solved for. The face-flux $\Phi^n_f = \left(\boldsymbol{\Psi}^{n-1}_f\cdot\boldsymbol{S}_f\right)$ is evaluated by using values from the previous outer iteration $n-1$. The interpolation of ϕ to face f of the control volume forms coefficients in the solution matrix, which get weighted with Φ^n_f. The `fvm::laplacian` operator works in a similar way:

$$\int_{V_{KV}} \nabla\cdot(\Gamma\nabla\phi)\,dV = \sum_f \Gamma^n_f\,(\nabla\phi)_f\cdot\boldsymbol{S}_f, \quad (10)$$

where Γ is a scalar. As shown in Table 1 several new terms of the ENSE are now discretized with these approaches. It should be noted here that by expanding $\nabla\cdot\left(\dot{\boldsymbol{m}}^D e\right)$ this can be done in both ways at once for the energy equation:

$$\begin{aligned}\nabla\cdot\left(\dot{\boldsymbol{m}}^D e\right) &= -\nabla\cdot\left[\left(\frac{\mu}{p}\nabla p\right)e\right] + \nabla\cdot\left(\frac{\mu e}{2T}\nabla T\right)\\ &= -\nabla\cdot\left[\left(\frac{\mu}{p}\nabla p\right)e\right] + \nabla\cdot\left(\frac{\mu C_V e}{2eC_V}\nabla e\right)\\ &= -\nabla\cdot\left[\left(\frac{\mu}{p}\nabla p\right)e\right] + \nabla\cdot\left(\frac{\mu}{2}\nabla e\right). \end{aligned} \quad (11)$$

The remaining new terms are discretized explicitly with corresponding operators from the `fvc` namespace. For an understanding of the discretization of the classical terms and OpenFOAM numerics in general also see Holzmann [18]. Special care is taken of the pressure equation, where the matrix assembly of $\nabla\cdot\dot{\boldsymbol{m}}^D$ has to be separated from the CNSE part (Step 6 and 7 in Fig. 2), as the convective flux would be otherwise corrected wrongly by the SIMPLE solution algorithm. Furthermore, the face normal component of $\dot{\boldsymbol{m}}^D$ is constrained to zero on the wall boundaries (Step 3 and 14 in Fig. 2). Hereby a diffusion through walls caused by a temperature gradient is prevented, which could occur when there is a constant temperature or a fixed heat flux as a boundary condition for the walls given. Fig. 2 shows the flow chart of the entire solution algorithm. The new solver is named rhoSimpleEnseFoam.

3. Illustrative example

Maurer et al. [19] performed experiments of a pressure-driven Helium flow through a rectangular microchannel for outlet Knudsen numbers of up to 1.5. Much higher mass flow rates than predicted by the CNSE could be observed. As proven by Sambasivam [10] the difference comes from the missing self-diffusive mass flux terms within the CNSE. Furthermore, in this case there are some characteristics of the ENSE solution regarding the pressure and velocity profiles that can be described by means of analytical formulas. These are now taken to verify the present OpenFOAM solver for this test case. Geometry, boundary conditions and material properties used are shown in Fig. 3 and Table 2. Originally they were adapted from Maurer et al. [19] with the exception of the channel height, which is taken to be 1.2 μm. Second-order discretization schemes are used for all terms. As this is an isothermal test case, solving the energy equation is omitted. It is felt that the extremely high aspect ratio causes general instabilities, especially with the unmodified rhoSimpleFoam. Therefore, convergence is achieved once the residuals drop below $1\cdot10^{-4}$. The case is run on one core. A meshing with 500 × 15 quadrilateral cells was found to be sufficient.

3.1. Performance observations

Depending on the pressure–velocity coupling algorithm, a meshing with 500 × 15 cells requires an underrelaxation of the density with $\alpha_\rho = 0.01$ (between Step 13 and 14 in Fig. 2) in order to achieve convergence, when the case is run on the isothermal version of the rhoSimpleFoam (CNSE) solver. Interestingly, the convergence is more easily achieved with the present rhoSimpleEnseFoam (ENSE) solver, where no such underrelaxation is required and the residuals can drop without any oscillations below $1\cdot10^{-6}$. Hereby it can be also observed that the implicit discretization of the pressure dependent part of $\nabla\cdot\dot{\boldsymbol{m}}^D$ is crucial for a performance gain compared to a purely explicit discretization of the new terms, i.e. by using only operators from the `fvc` namespace. Doing the latter would make an underrelaxation of the pressure with $\alpha_p = 0.0002$ (Step 12 in Fig. 2) necessary, which in turn increases the number of iterations to

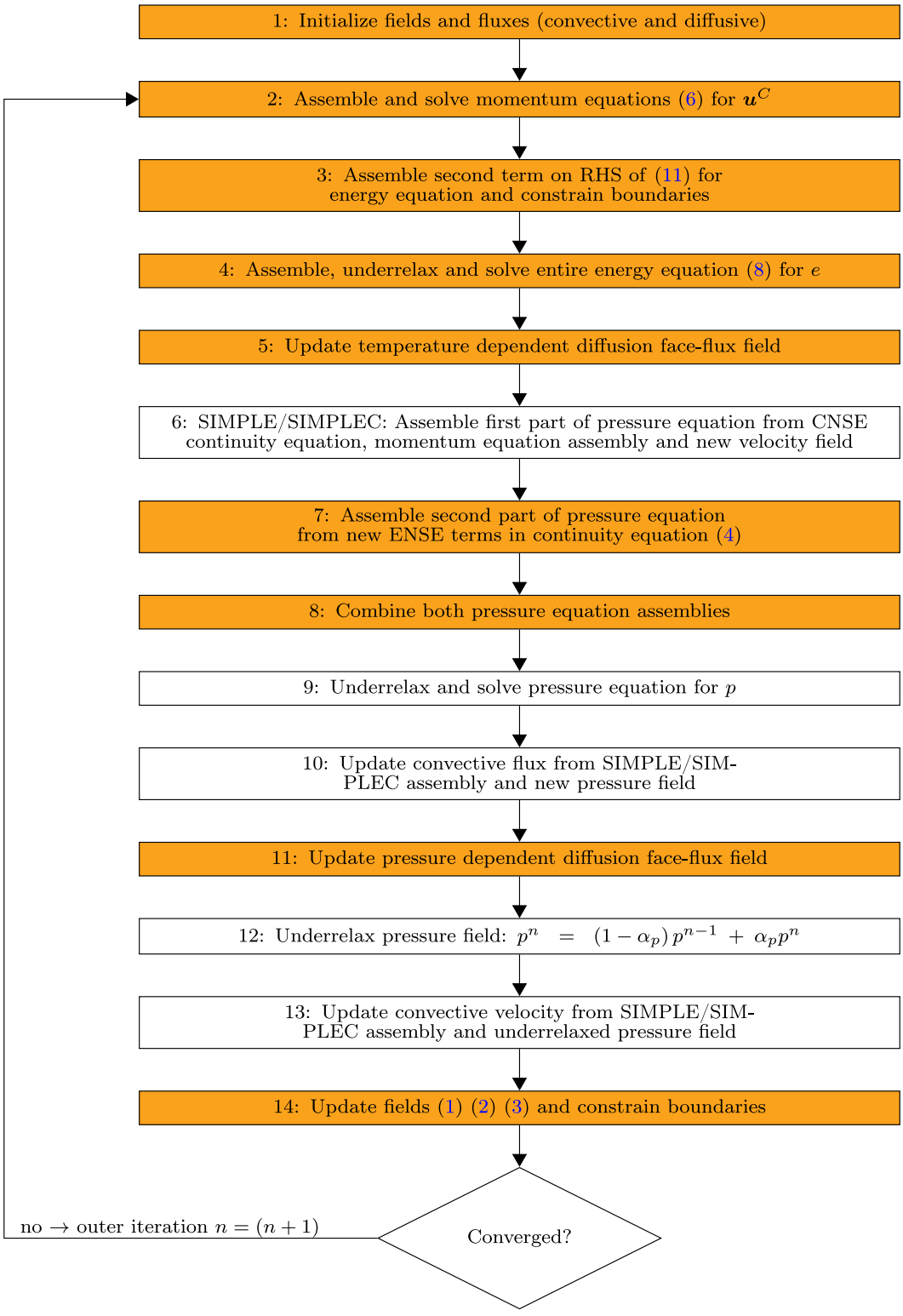


Fig. 2. Flowchart of the rhoSimpleEnseFoam solver algorithm. Orange colored parts are either modified or completely new compared to rhoSimpleFoam. (For interpretation of the references to color in this figure legend, the reader is referred to the web version of this article.)

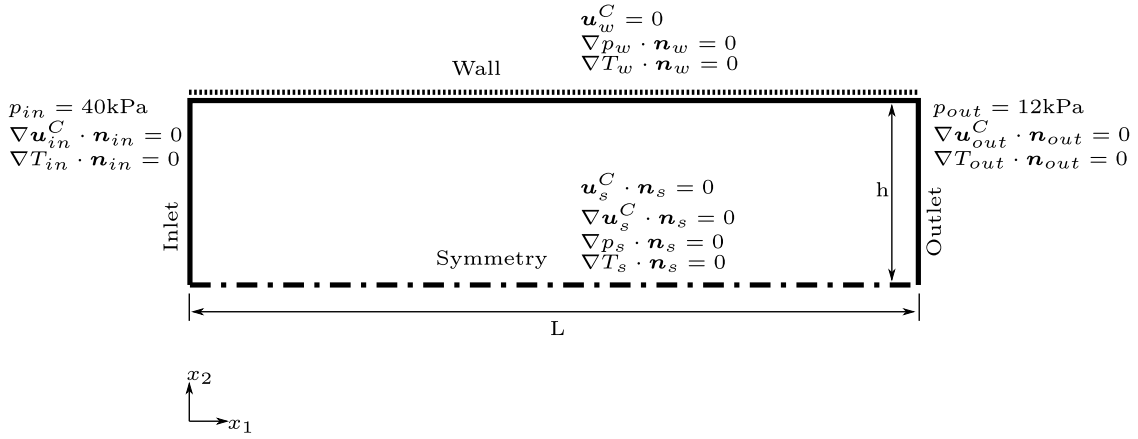


Fig. 3. Geometry and boundary conditions for the verification test case. The subscripts denote an arbitrary surface patch element on the corresponding boundary, while $\boldsymbol{n}$ is the surface normal unity vector.

Table 1
New terms of the ENSE that are discretized implicitly.

Equation	ϕ	Term	OpenFOAM operator	Γ_f^n/Φ_f^n
Continuity (4)	p	$\nabla \cdot \left(\frac{-\mu}{p}\nabla p\right)$	`fvm::laplacian`	$\left(-\frac{\mu}{p^{n-1}}\right)_f$
Momentum (6)	$\boldsymbol{u}^C$	$\nabla \cdot \left(\boldsymbol{u}^C \dot{\boldsymbol{m}}^D\right)$	`fvm::div`	$\dot{\boldsymbol{m}}_f^{D,n-1} \cdot \boldsymbol{S}_f$
Energy (8)	e	$-\nabla \cdot \left[\left(\frac{\mu}{p}\nabla p\right) e\right]$	`fvm::div`	$\left(-\frac{\mu}{p^{n-1}}\nabla p^{n-1}\right)_f \cdot \boldsymbol{S}_f$
		$\nabla \cdot \left(\frac{\mu}{2}\nabla e\right)$	`fvm::laplacian`	$\left(\frac{\mu}{2}\right)_f$

Table 2
Material properties for the microchannel test case [10] and OpenFOAM solver parameters.

Parameter	Simulation	Maurer et al. [19]
Channel height $H = 2h$ [μm]	1.2	1.14
Width [μm]	200	200
Length L [mm]	10	10
Domain temperature [K]	293	293
Gas	Helium	Helium
Gas constant $[\frac{\text{J}}{\text{Kg K}}]$	2077	2077
Gas viscosity [10^{-5} Pa s]	1.99	1.99
Outlet Knudsen number Kn_{out}	1.509	$1.509 - 0.179$
Iterative solver — pressure equation	GAMG	–
Iterative solver — momentum equation	PBiCGStab	–
Iterative solver — energy equation	PBiCGStab	–

achieve convergence by a factor of around 3.3. This is broadly in agreement with the findings of Sambasivam [10], who employed User-Defined-Functions (UDF) in ANSYS Fluent for solving the ENSE. He attributed the bad convergence behavior in case of large Knudsen numbers to the fact that the new terms are only implemented as source terms. Fig. 4 shows the graph of the residuals for each of the mentioned solvers.

3.2. Verification of the results

The pressure profiles along the channel length in Fig. 5 from both the CNSE and ENSE solver are plotted together with the analytical ENSE solution, derived by Jaishankar and McKinley [20]:

$$p(x_1) = P\sqrt{W\left[exp\left(-\frac{p_{out}^2}{P^2}\left(\frac{p_{in}^2}{p_{out}^2} - 1 + \frac{P^2}{p_{out}^2}\ln\left(\frac{p_{in}}{p_{out}}\right)\right)\frac{x_1}{L}\frac{p_{in}^2}{P^2} + \ln\left(\frac{p_{in}^2}{P^2}\right)\right)\right]}, \tag{12}$$

with W being the Lambert W function and $P = \mu\sqrt{3RT}/h$ the characteristic pressure. ENSE numerics and analytics are in good agreement, yet a small deviation is visible. This might be due to the simplifications that were made during the derivation of Eq. (12). It can be observed that the CNSE solution has a concave downward curvature. As the pressure and therefore the density decreases towards the outlet, the velocity has to increase because the mass flow rate has to be equal at all positions in the channel. This causes the shear forces and hence the local pressure-drop to rise towards the outlet. On the other hand, the solution of the ENSE is curved upwards. It can be deduced from Eq. (1) that a decrease of pressure causes an increase of the self-diffusive mass flux, which leads to a decreasing convective flux because the continuity equation has to be fulfilled. Since the convective mass flux is a result of local pressure gradients, their magnitude decrease towards the outlet as well. This behavior is just the case in areas where the diffusive mass flux is the dominant driving mechanism of the flow. In regions where the convective flux would dominate, the curvature is concave downward here too as it was proven by Sambasivam [10].

The profile of the velocity profiles obtained with rhoSimpleFoam (CNSE) and the present rhoSimpleEnseFoam (ENSE) at two different locations in the channel is plotted over the cross section in Fig. 6 along with the following analytical solution (ENSE) [10]:

$$u_1(x_1, x_2) = -\frac{1}{2\mu}\frac{\partial p}{\partial x_1}(h^2 - x_2^2) - \frac{\mu}{\rho}\left(\frac{1}{p}\frac{\partial p}{\partial x_1}\right), \tag{13}$$

where the first part represents the parabolic profile of the convective velocity and the last term is the block profile of the diffusive velocity. Analytics and numerics fit very well. The total ENSE-velocity has a slip-like offset caused by the diffusive velocity. As already mentioned, the ratio $\boldsymbol{u}^D/\boldsymbol{u}^C$ tends to increase towards the outlet as the pressure drops. Furthermore, $\boldsymbol{u}^D$ is constant along

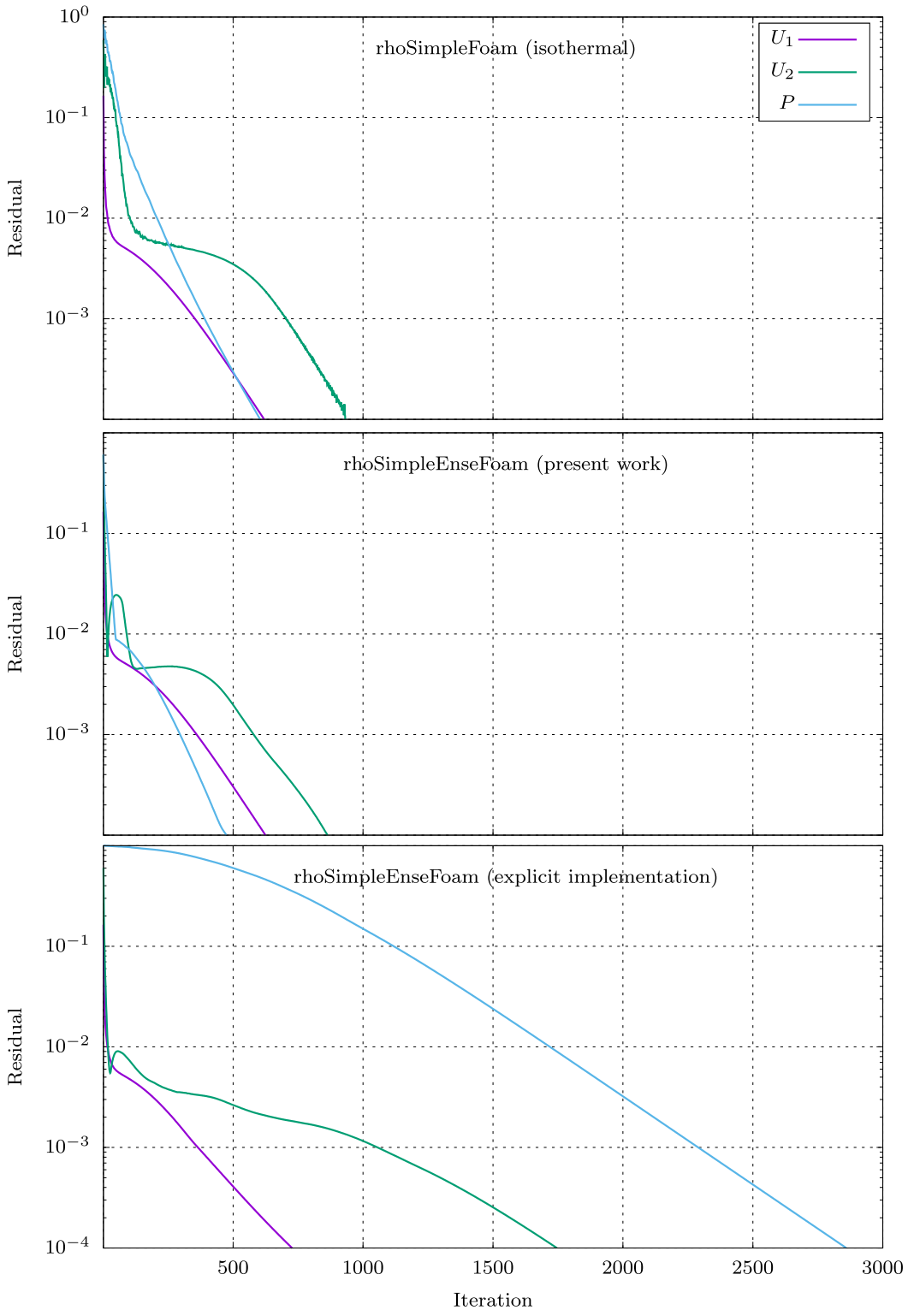


Fig. 4. Graph of residuals for the different solvers used in the test case plotted over the number of outer iterations. The explicit implementation requires a heavy underrelaxation of the pressure.

the cross section of the channel because the pressure gradient does not change there either.

4. Impact and conclusion

An OpenFOAM solver for the ENSE by Durst et al. [7–9] has been implemented in this work. The OpenFOAM source code allows the implicit discretization of several of the new terms. This results in a far better performance than with a purely explicit discretization. Using a simple test case with a rectangular geometry the results have been verified against analytical formulas. However, as this is just an isothermal test case with a simple geometry, deeper investigations for performance and accuracy would require a more sophisticated case. Nevertheless, the

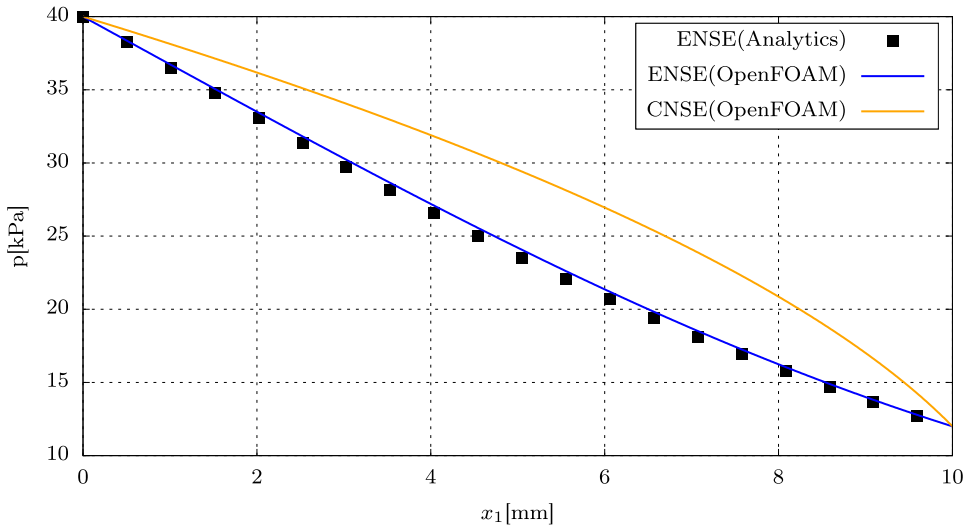


Fig. 5. Pressure profiles plotted over the channel length x_1. Comparison between rhoSimpleFoam(CNSE), rhoSimpleEnseFoam(ENSE) and analytics(ENSE).

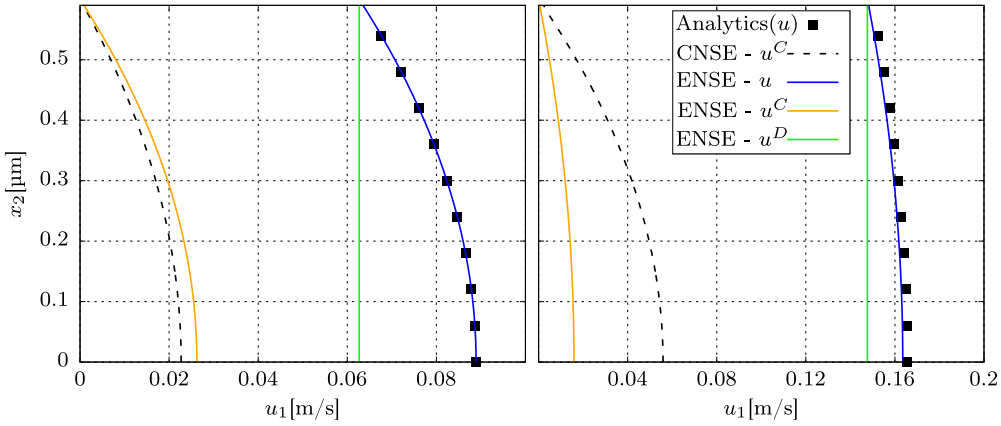


Fig. 6. Profile of the velocity components plotted over the channels cross section at the middle of the channel at $x_1 = 5$ mm (left figure) and at the outlet at $x_1 = 10$ mm (right figure), obtained from rhoSimpleFoam(CNSE), rhoSimpleEnseFoam(ENSE) and analytics(ENSE).

solver gives a starting point to anyone who wants to numerically investigate these equations. Possible areas of interest could be thermal transpiration [10], thermophoresis [10], cold-to-hot heat transfer [21,22], flows involving more complex geometries and – although it might require a density-based approach – hypersonic shock structures [5,6]. Furthermore, the solver can be extended by the use of Maxwell slip boundary conditions and models for an effective mean free path [12,23,24] in order to efficiently simulate gas flows with $Kn \gg 1$.

Declaration of competing interest

The authors declare that they have no known competing financial interests or personal relationships that could have appeared to influence the work reported in this paper.

Data availability

Data will be made available on request

References

[1] Brenner Howard. Navier–Stokes revisited. Physica A 2004;349:60–132. http://dx.doi.org/10.1016/j.physa.2004.10.034.
[2] Brenner Howard. Beyond Navier-Stokes. Internat J Engrg Sci 2012;54:67–98. http://dx.doi.org/10.1016/j.ijengsci.2012.01.006.
[3] Christou Chariton, Dadzie S Kokou. On the numerical simulation of rarefied gas flows in micro-channels. J Phys Commun 2018;2. http://dx.doi.org/10.1088/2399-6528/aab066.
[4] Ewart Timothée, Perrier Pierre, Graur Irina A, Méolans J Gilbert. Mass flow rate measurements in a microchannel, from hydrodynamic to near free molecular regimes. J Fluid Mech 2007;584:337–56. http://dx.doi.org/10.1017/S0022112007006374.
[5] Greenshields CJ, Reese JM. The structure of shock waves as a test of Brenner's modifications to the Navier-Stokes equations. J Fluid Mech 2007;580:407–29. http://dx.doi.org/10.1017/S0022112007005575.
[6] Greenshields C J, Reese J M. The structure of hypersonic shock waves using Navier-Stokes equations modified to include mass diffusion. In: 2nd European conference on aerospace sciences. 2007.
[7] Durst F, Gomes J, Sambasivam R. Thermofluiddynamics: Do We Solve the Right Kind of Equations? In: Turbulence heat and mass transfer 5. Proceedings of the international symposium on turbulence heat and mass transfer. 2006, http://dx.doi.org/10.1615/ICHMT.2006.TurbulHeatMassTransf.10.
[8] Chakraborty Suman, Durst Franz. Derivations of extended Navier-Stokes equations from upscaled molecular transport considerations for compressible ideal gas flows: Towards extended constitutive forms. Phys Fluids 2007;19. http://dx.doi.org/10.1063/1.2759531.
[9] Durst F, Filimonov D, Sambasivam R. Treatments of micro-channel flows revisited: Continuum versus rarified gas considerations. J Inst Eng (India): Ser C 2020;101. http://dx.doi.org/10.1007/s40032-020-00586-3.
[10] Sambasivam Rajamani. Erweiterte Navier-Stokes-Gleichungen: Ableitungen und Anwendungen auf Strömungsprobleme (Ph.D. thesis), Friedrich-Alexander-Universität Erlangen-Nürnberg; 2012.
[11] Moukalled Fadl, Darwish Marwan, Mangani Luca. The finite volume method in computational fluid dynamics an advanced introduction with OpenFOAM(R) and Matlab (fluid mechanics and its applications). Springer-Verlag; 2015.

[12] Jaiswal Shashank, Dongari Nishanth. Implementation of Knudsen layer effects in open source CFD solver for effective modeling of microscale gas flows. In: Proceedings of the 23rd national heat and mass transfer conference and 1st international ISHMT-ASTFE heat and mass transfer conference. 2015.
[13] Bhagat Apurva, Gijare Harshal, Dongari Nishanth. Modeling of Knudsen layer effects in the micro-scale backward-facing step in the SlipFlow Regime. Micromachines 2019;10. http://dx.doi.org/10.3390/mi10020118.
[14] Greenshields Christopher J, Weller Henry G, Gasparini Luca, Reese Jason M. Implementation of semi-discrete, non-staggered central schemes in a colocated, polyhedral, finite volume framework, for high-speed viscous flows. Internat J Numer Methods Fluids 2010;63:1–21. http://dx.doi.org/10.1002/fld.2069.
[15] Kraposhin Matvey, Banholzer Matthias, Pfitzner Michael, Marchevsky Ilia K. A hybrid pressure-based solver for nonideal single-phase fluid flows at all speeds. Internat J Numer Methods Fluids 2018;88:79–99. http://dx.doi.org/10.1002/fld.4512.
[16] Heinrich Martin, Schwarze Rüdiger. Density-based solver for all Mach number flows. Progress Comput Fluid Dyn Int J 2016;271–80. http://dx.doi.org/10.1504/PCFD.2016.078752.
[17] Greenshields Christopher J. OpenFOAM Programmers Guide. 2015.
[18] Holzmann Tobias. Mathematics, Numerics, Derivations and OpenFOAM. 2020.
[19] Maurer Jean, Tabeling Patrick, Joseph Pierre, Willaime Herve. Second-order slip laws in microchannels for helium and nitrogen. Phys Fluids 2003;15:2613–21. http://dx.doi.org/10.1063/1.1599355.
[20] Jaishankar Aditya, McKinley Gareth H. An analytical solution to the extended Navier–Stokes Equations using the Lambert W function. AIChE J 2014;60:1413–23. http://dx.doi.org/10.1002/aic.14407.
[21] Mahdavi Amir-Mehran, Roohi Ehsan. Investigation of cold-to-hot transfer and thermal separation zone through nano step geometries. Phys Fluids 2015;27. http://dx.doi.org/10.1063/1.4927069.
[22] Ebrahimi Amin, Shahabi Vahid, Roohi Ehsan. Pressure-driven nitrogen flow in divergent microchannels with isothermal walls. Appl Sci 2021;11(8).
[23] Dongari Nishanth, Durst F, Chakraborty Suman. Predicting microscale gas flows and rarefaction effects through extended Navier–Stokes–Fourier equations from phoretic transport considerations. Microfluid Nanofluid 2010;9:831–46. http://dx.doi.org/10.1007/s10404-010-0604-5.
[24] Lockerby Duncan A, Reese Jason M, Gallis Michael A. Capturing the Knudsen layer in continuum-fluid models of nonequilibrium gas flows. AIAA J 2005;43(6):1391–3. http://dx.doi.org/10.2514/1.13530.